

**Diffraction of acoustic waves
from a point source over an impedance
wedge**

Mikhail A. Lyalinov

St. Petersburg University

Universitetskaya nab. 7/9

199034, Saint-Petersburg, Russia¹⁾

URSI GA 2020

¹⁾Email: lyalinov@yandex.ru, m.lyalinov@spbu.ru

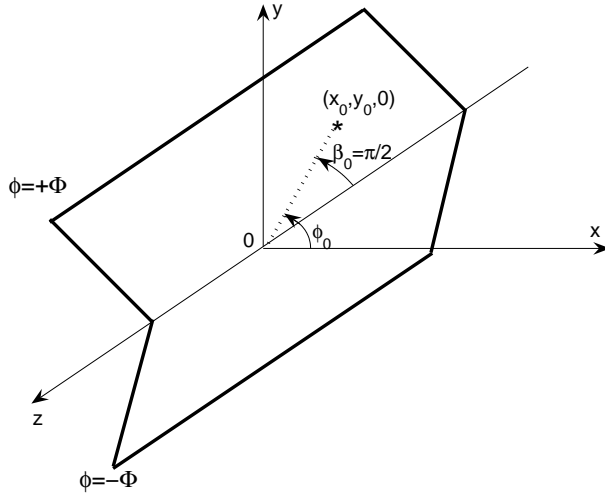


Figure 1: Diffraction of waves from a point source over an impedance wedge

1 Statement of the problem

In the exterior Ω of a wedge with the surface S consisting of two faces S_+ and S_- (Fig. 1) the acoustic wave field u (Green's function) satisfies the Helmholtz equation

$$(\Delta + k^2)u(X, Y, Z) = -\delta(X - x_0)\delta(Y - y_0)\delta(Z), \quad (1)$$

where the point source is located at $(x_0, y_0, 0)$.

The impedance boundary conditions on the wedge's faces S_{\pm}

$$\left(\pm \frac{1}{r} \frac{\partial u}{\partial \varphi} - ik\eta_{\pm} u \right) \Big|_{\varphi=\pm\Phi} = 0, \quad (2)$$

where $k > 0$, $\pi/2 < \Phi \leq \pi$, η_{\pm} are the surface impedances.

Meixner's condition, as $r \rightarrow 0$,

$$u(r, \varphi, z) = C + O(r^{\delta}), \quad \delta > 0. \quad (3)$$

Radiation condition at infinity

$$\int_{S_R} \left| \frac{\partial u}{\partial r} - ik u \right|^2 ds \rightarrow 0, \quad \text{as } r = R \rightarrow \infty, \quad (4)$$

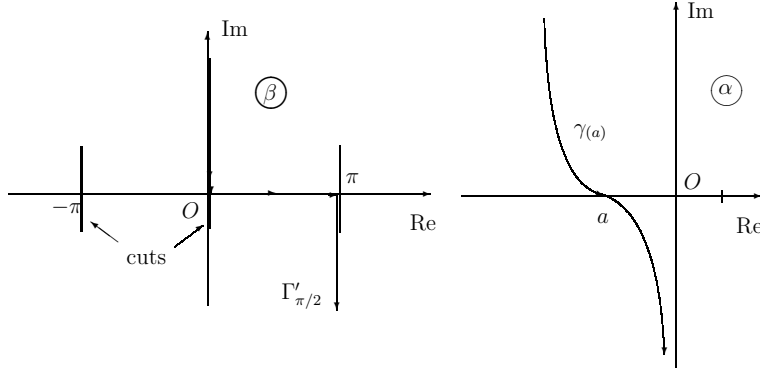


Figure 2: The contours of integration for the Weyl integrals for the wave field from the point source. The branch cuts for $\theta^+(\beta)$ connect the points $\arcsin \eta_+ + \pi n$ and $-\arcsin \eta_+ + \pi n$ with $n = 0, \pm 1, \dots$ correspondingly.

1.1 Integral representations of the wave field

Weyl integral representation. We make use of the integral representation for the incident field from an acoustic point source in 3D space located at $M_0 = (x_0, y_0, 0)$

$$u_0(M) = \frac{ik}{8\pi^2} \int_{\Gamma_{\pi/2}} d\beta \int_{\gamma_{\psi-\pi}} d\alpha \sin \beta e^{ik[z \cos \beta + \sin \beta (r_0 \cos(\alpha-\varphi_0) - r \cos(\alpha-\varphi))]} \quad (5)$$

and also $u_0(M) = \frac{e^{ikR_0}}{4\pi R_0}$, where $M = (X, Y, Z)$ (or (r, φ, z)), $R_0 = |MM_0|$, the contours of integration in (5) are shown in Fig. 2, ($0 \leq \psi < 2\pi$).²⁾

The total field from the point source over a wedge is sought in an analogous form

$$u(M) = \frac{ik}{8\pi^2} \int_{\Gamma'_{\pi/2}} d\beta \int_{\gamma(\varphi_0)} d\alpha \sin \beta e^{ik[z \cos \beta + \sin \beta r_0 \cos(\alpha-\varphi_0)]} U(r, \varphi; \alpha, \beta) \quad (6)$$

with yet unknown $U(r, \varphi; \alpha, \beta)$ and with the contours of integration shown in Fig.

²⁾ The contour $\Gamma_{\pi/2}$ coincides with $\Gamma'_{\pi/2}$ in Fig 2., however, the integrand in (5) does not have any branching points.

2, $\Gamma'_{\pi/2} = (i\infty, 0+] \cup [0+, \pi - 0] \cup [\pi - 0, \pi - 0 - i\infty)$.

$$U(r, \varphi; \alpha, \beta) = \frac{1}{2\pi i} \int_{\gamma} ds e^{-ikr \sin \beta \cos s} f(s + \varphi; \alpha, \beta), \quad (7)$$

where the double-loop Sommerfeld contour of integration γ is shown in Fig. 1.1 together with the steepest descent paths (SDP), the function f is specified by the expressions

$$f(s; \alpha, \beta) = \frac{\mu \cos \mu \alpha}{\sin \mu s - \sin \mu \alpha} \frac{\Psi(s; \beta)}{\Psi(\alpha; \beta)}, \quad \mu = \frac{\pi}{2\Phi}$$

and

$$\Psi(s; \beta) =$$

$$\psi_{\Phi}(s - \Phi + \pi/2 - \vartheta^-(\beta)) \psi_{\Phi}(s - \Phi - \pi/2 + \vartheta^-(\beta)) \psi_{\Phi}(s + \Phi + \pi/2 - \vartheta^+(\beta)) \psi_{\Phi}(s + \Phi - \pi/2 + \vartheta^+(\beta)).$$

The meromorphic function $\psi_{\Phi}(\cdot)$ is the Malyuzhinets function (see [?], Sect. 6.2).

The Malyuzhinets function is a meromorphic solution of the functional difference equation

$$\frac{\psi_{\Phi}(z + 2\Phi)}{\psi_{\Phi}(z - 2\Phi)} = \cot \left(\frac{z}{2} + \frac{\pi}{4} \right)$$

and in the strip $|\Re(z)| < \pi/2 + 2\Phi$ has an integral representation

$$\psi_{\Phi}(z) = \exp \left[-\frac{1}{2} \int_0^{\infty} \frac{\cosh(z\zeta) - 1}{\zeta \cosh(\pi\zeta/2) \sinh(2\Phi\zeta)} d\zeta \right].$$

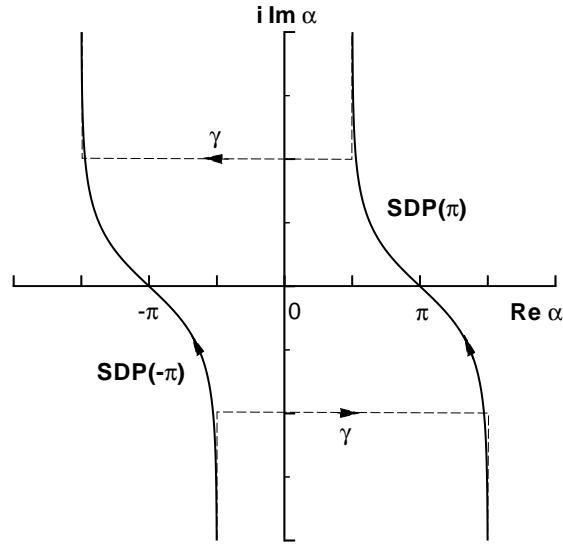


Figure 3: The plane of the complex variable s with the Sommerfeld double loops γ and the steepest descent paths $\gamma_{\pm\pi} := SDP(\pm\pi)$

2 The far-field asymptotics: the point source is not close to the wedge's faces

2.1 The incident field from the source, the reflected waves

$$u_0(M) = \frac{e^{ikR_0}}{4\pi R_0} \quad (8)$$

as $|\varphi - \varphi_0| < \pi$, otherwise, there is no contribution from the saddle point, $u_0(M) = 0$.

The reflected waves

$$u_{\pm}^r(M) = R^{\pm}(\alpha_0^{\pm}, \beta_0^{\pm}) \frac{e^{ik\psi^{r\pm}}}{4\pi\psi^{r\pm}} \quad (9)$$

as $|\pm 2\Phi - \varphi - \varphi_0| < \pi$, otherwise, $u_{\pm}^r(M) = 0$. The reflected waves can be interpreted as the waves emanated by the imaginary sources which are the mirror images of the real source at $(x_0, y_0, 0)$ w.r.t. the wedge's faces S_{\pm} , $R^{\pm}(\alpha_0^{\pm}, \beta_0^{\pm})$ are the reflection coefficients, see Appendix. The eikonals of these waves are $\psi^{r\pm}$ correspondingly.

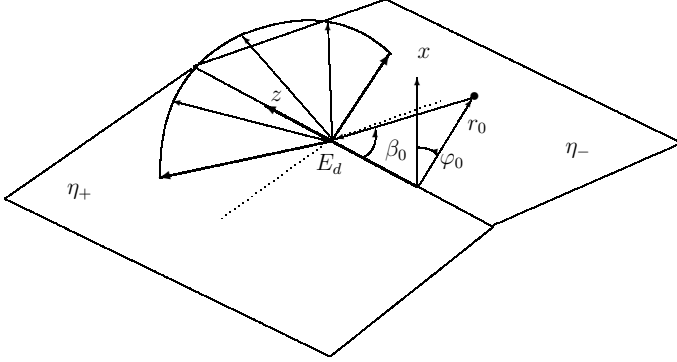


Figure 4: The edge wave and Keller's cone

2.2 The space wave, excited by the incident space wave, from the edge

Applying the formula for the leading term in the 3D steepest descent technique

$$u^e(M) = \frac{e^{i\pi/4}}{4\pi} \frac{e^{ik\sqrt{z^2+(r+r_0)^2}}}{\sqrt{(z^2+(r+r_0)^2)}} \left\{ \frac{\sqrt{z^2+(r+r_0)^2}}{2\pi k r r_0} \right\}^{1/2} \mathcal{D}(\varphi, \varphi_0, \beta_0) \left(1 + O\left(\frac{1}{k}\right) \right), \quad (10)$$

where $\mathcal{D}(\varphi, \varphi_0, \beta_0) = f(-\pi + \varphi; \varphi_0, \beta_0) - f(\pi + \varphi; \varphi_0, \beta_0)$ is the diffraction coefficient of the edge wave.

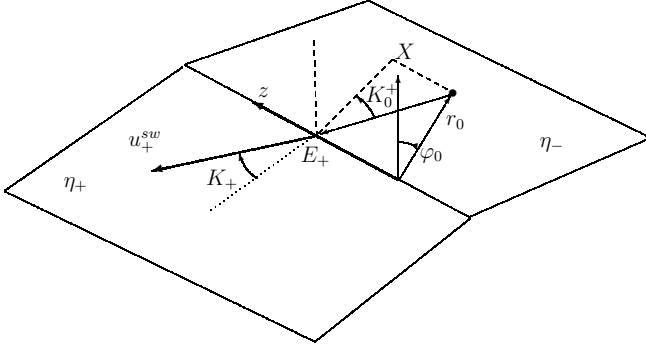


Figure 5: Surface waves from the edge.

2.3 Surface waves propagating from the edge

$$u_{\pm}^{sw}(M) = \sin \beta_0^{\pm} C^{\pm}(\varphi_0, \beta_0^{\pm}) \frac{e^{-ikr \sin(\Phi \mp \varphi) \eta^{\pm}}}{4\pi} \times$$

$$\frac{\exp(ik[z \cos \beta_0^{\pm} + \sin \beta_0^{\pm} r_0 \cos(\alpha - \varphi_0) + \sqrt{\sin^2 \beta_0^{\pm} - \eta_{\pm}^2} r \cos(\Phi \mp \varphi)])}{\left\{ \frac{r_0^2}{\sin^2 \beta_0^{\pm}} + \frac{r_0 r \cos[\Phi \mp \varphi]}{\sin^2 \beta_0^{\pm} - \eta_{\pm}^2} \frac{\sin \beta_0^{\pm}}{\sqrt{\sin^2 \beta_0^{\pm} - \eta_{\pm}^2}} \right\}^{1/2}} \left(1 + O\left(\frac{1}{k}\right) \right). \quad (11)$$

The expressions in (11) are really present in the asymptotics if the observation point is close to the wedge's face $\varphi = \pm\Phi$ correspondingly or, more exactly, as $0 < \Phi \mp \varphi < -\text{gd}(\text{Im} \vartheta^{\pm}(\beta_0^{\pm}))$.

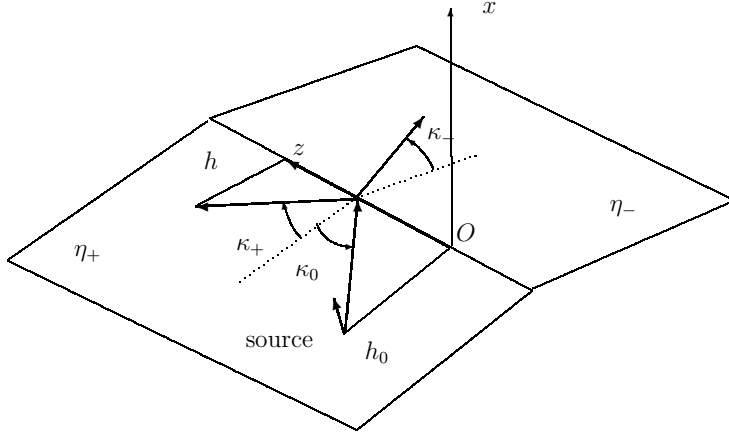


Figure 6: Reflection and transmission of the primary surface wave at the edge, $h = r \cos[\Phi - \varphi]$,
 $h_0 = r_0 \cos[\Phi - \varphi_0]$

3 Reflection and transmission of the primary surface wave at the edge of the wedge

The primary surface wave propagates to the edge and gives rise to the edge wave and to the reflected and transmitted surface wave. In the leading approximation, for the reflected surface wave we find

$$u_r^{sw}(M) = r_{\vartheta+}(\tau_+) \times \frac{k e^{i3\pi/4}}{2\sqrt{2\pi}} \frac{e^{ik[r_0 \sin(\varphi_0 - \Phi)\eta_+ + r \sin(\varphi - \Phi)\eta_+]}}{\sqrt{(1 - \eta_+^2)k\rho}} \left\{ \frac{1 - \eta_+^2}{1 + z^2/\rho^2} \right\}^{3/4} e^{ik\sqrt{(1 - \eta_+^2)(z^2 + \rho^2)}} \left(1 + O\left(\frac{1}{k}\right) \right). \quad (12)$$

In a similar manner we deal with the transmitted surface wave. The Snel's type law of refraction of the primary surface wave across the edge of two impedance halfplanes reads

$$\sqrt{1 - \eta_+^2} \sin \kappa_+ = \sqrt{1 - \eta_-^2} \sin \kappa_-.$$

The leading term of the transmitted surface wave takes the form

$$u_t^{sw}(M) = r_{\vartheta-}(\tau_-) \frac{k e^{i3\pi/4}}{2\sqrt{2\pi}} \frac{e^{ik[r_0 \sin(\varphi_0 - \Phi)\eta_- + r \sin(\varphi - \Phi)\eta_-]}}{\sqrt{k\rho}} \times$$

$$\left\{ \frac{\gamma^+(1-\eta_+^2)\tau_-}{[\sqrt{1-\eta_+^2-\tau_-^2}]^3} + \frac{\gamma^-(1-\eta_-^2)\tau_-}{[\sqrt{1-\eta_-^2-\tau_-^2}]^3} \right\}^{-1/2} e^{ik[z\tau_- + \rho\gamma^+\sqrt{1-\eta_+^2-\tau_-^2} + \rho\gamma^-\sqrt{1-\eta_-^2-\tau_-^2}]} \left(1 + O\left(\frac{1}{k}\right) \right). \quad (13)$$

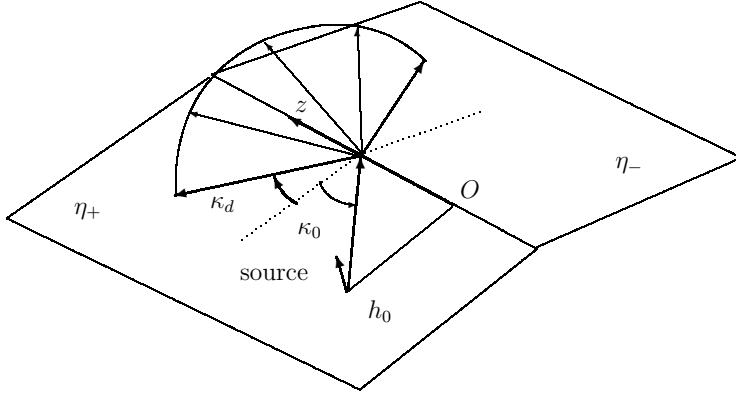


Figure 7: The edge wave generated by the primary surface wave

4 The edge wave generated by the primary surface wave interacting with the edge

The expression for this wave is also obtained by means of the asymptotic evaluation of the integral that originates from the residue of $f(s + \pi + \varphi; \alpha, \beta) - f(s - \pi + \varphi; \alpha, \beta)$ of the integrand. We find

It is worth noticing the existence of the critical angle κ_0^* for edge wave which corresponds to $\kappa_d = \pi/2$,

$$\kappa_0^* = \arctan\left(\frac{1}{|\eta_+|}\right).$$

For this angle the edge wave collapses to be concentrated near the edge. The point τ_e goes to the branch points of $\sqrt{1 - \tau^2}$ and disappears through the cut. The asymptotics of the integral, in this case, requires a special study. For the electromagnetic case some additional details can be found in [?].

The leading term of the asymptotics reads ($\tau_e = \cos \beta_e$)

$$u_e^{sw}(M) = \frac{d(\tau_e, 0; \varphi)}{4\pi} \left\{ \frac{r^2}{\sin^2 \beta_e} + r r_0 \cos[\Phi - \varphi_0] \frac{(1 - \eta_+^2) \sin \beta_e}{\sqrt{\sin^2 \beta_e - \tau_e^2}} \right\}^{-1/2} e^{-i k r_0 \sin(\Phi - \varphi_0) \eta_+} e^{i k [z \cos \beta_e + \sin \beta_e r + r_0 \cos(\Phi - \varphi_0) \sqrt{\sin^2 \beta_e - \eta_+^2}]} \left(1 + O\left(\frac{1}{k}\right) \right). \quad (14)$$

5 Conclusion

In this paper, we applied recently developed results [1] (Chapter 3), [2],[3], obtained in the case of electromagnetic problem, to the acoustic one. A principal difference of the acoustic case is that, contrary to the electromagnetic problem which requires solution of an integral equation, it is explicitly solvable. The corresponding non-uniform asymptotic results are written in terms of the Malyuzhinets' and elementary functions. The Weyl integral representation played a crucial role, whereas the integrand was found explicitly in terms of the Malyuzhinets' solution of an auxiliary problem.

We could obtain asymptotic components of the total field as $k \rightarrow \infty$. In this way, as a result of asymptotic evaluation of the integrals we also clarified physical meaning of the wave components computed. In particular, the laws of the Geometrical Theory of Diffraction describing the interaction of the primary surface wave with the edge were discussed.

One of the further prospects is in study of possible excitation of the edge waves, i.e. the waves whose energy is concentrated near the edge. Such localized waves, together with the other waves, might actually propagate along the edge in the opposite directions from the source located near the edge. To our mind, existence of such phenomenon can be expected, for instance, provided the impedances of the faces coincide and the wedge's opening 2Φ is less than π . Remark that the existence and excitation of the edge waves in elasticity is also of great practical importance.

References

- [1] M. A. Lyalinov and N. Y. Zhu, *Scattering of Waves by Wedges and Cones with Impedance Boundary Conditions* (Mario Boella Series on Electromagnetism in Information & Communication). Edison, NJ: SciTech-IET, (2012).

- [2] M. A. Lyalinov and N. Y. Zhu, “ Electromagnetic Scattering of a Dipole-Field by an Impedance Wedge, Part I: Far-Field Space Waves ,” *IEEE Trans. Antennas Propag.*, vol. 61 , no. 1, pp. 329-337, 2013.
- [3] M. A. Lyalinov and N. Y. Zhu, “ Scattering of an electromagnetic surface wave from a Hertzian dipole by the edge of an impedance wedge, ” *Journal of Mathematical Sciences*, vol. 226 , no. 6, pp. 768-778, 2017. (<https://doi.org/10.1007/s10958-017-3565-3>)
- [4] M. A. Lyalinov and N. Y. Zhu, “Diffraction of a skew incident plane electromagnetic wave by an impedance wedge,” *Wave Motion*, vol. 44, no. 1, pp. 21-43, Nov. 2006.
- [5] M. A. Lyalinov and N. Y. Zhu, “Diffraction of a skew incident plane electromagnetic wave by a wedge with axially anisotropic impedance faces,” *Radio Sci.*, vol. 42, no. 6, RS6S03, 2007.